Journal of Crop Science and Biotechnology
https://doi.org/10.1007/s12892-026-00363-1

RESEARCH

Next generation sequencing-based MutMap identifies genomic regions associated with strong culm in rice

Pritam Kanti Guha[1,2] · Anil A. Hake[1,3] · Kalyani M. Barbadikar[1] · Potupureddi Gopi[1,4] · Nakul D. Magar[1] · Vishalakshi Balija[1] · C. G. Gokulan[5,6] · Madhavilatha Kommana[1,3] · Md Jamaloddin[5] · Anjana Sharma[5,7] · Raju Madanala[5] · A. Chandra Sekhar[2] · D. Vijaya Raghava Prasad[2] · D. Vijaya Lakshmi[2] · Hitendra Kumar Patel[5,7] · Ramesh Venkata Sonti[5,8] · Sundaram Raman Meenakshi[1] · Sheshu Madhav Maganti[1,3]

Received: 23 December 2025 / Accepted: 2 June 2026
© The Author(s), under exclusive licence to Korean Society of Crop Science (KSCS) 2026

Abstract
Culm strength is a key determinant of lodging resistance in rice, directly impacting yield stability and resilience. To identify genomic regions associated with strong culm, we characterized the strong culm mutant TI-17, derived from the Indian mega rice variety *Samba Mahsuri (BPT-5204)*. Comparative anatomical analyses revealed that TI-17 exhibited increased culm wall thickness, sclerenchyma thickness, and xylem vessel sclerenchyma thickness, along with a reduced xylem vessel diameter relative to BPT-5204. Using the MutMap approach, we identified 12 candidate genes distributed across three genomic regions on chromosomes 3 (32.71–33.70 Mb), 4 (18.2–20.0 Mb), and 8 (24.0–27.0 Mb). SNPs within the candidate regions were converted into KASP assays, including KASP8_9 (chr8:26248706; A→G; CAG [Glutamine] to CGG [Arginine]) in *Os08g0527300*, encoding peptidase C19, ubiquitin carboxyl-terminal hydrolase 2 domain containing protein. This SNP of KASP8_9 demonstrated perfect co-segregation with culm strength, effectively differentiating weak and strong culm genotypes. The findings highlight *Os08g0527300* as a promising target for the genetic improvement of culm strength, contributing to the development of high-yield, climate-resilient rice varieties.

Keywords Rice · MutMap · Strong culm · KASP · qRT-PCR

Introduction

Induced mutagenesis is a vital method that enhances crop genetic variability, addressing the limitations of a narrow genetic base and aiding structural genomics. In rice, several traits and genes have been identified through mutation breeding, including *Dwarf 1* (*D1*) for dwarfness, *qSH3* for seed shattering, *OSH15* for tillers, *OsHAC4* for arsenic tolerance, *oscyp96b4* for semi-dwarfness, and *Osnop* for pollen sterility. In current study, we have utilized stabilized mutants imparting strong culm trait generated by ethyl methane sulphonate (EMS)-mutagenized seeds of BPT-5204.

✉ Kalyani M. Barbadikar
kalyaniaau@gmail.com

✉ D. Vijaya Lakshmi
dvlyvu@yvu.edu.in

✉ Sheshu Madhav Maganti
sheshu24@gmail.com

Anil A. Hake
anilhake30@gmail.com

[1] ICAR-Indian Institute of Rice Research, Hyderabad, Telangana 500030, India

[2] Department of Microbiology, Yogi Vemana University, YSR Kadapa, Andhra Pradesh 516005, India

[3] ICAR-National Institute for Research on Commercial Agriculture, Rajahmundry, Andhra Pradesh 533105, India

[4] International Crops Research Institute for the Semi-Arid Tropics, Patancheru, Hyderabad, Telangana 502324, India

[5] CSIR-Centre for Cellular and Molecular Biology, Hyderabad, Telangana 500007, India

[6] Department of Plant-Microbe Interactions, BRIC-Centre for DNA Fingerprinting and Diagnostics, Hyderabad, Telangana 500039, India

[7] Academy of Scientific and Innovative Research (AcSIR), Ghaziabad 201002, India

[8] International Centre for Genetic Engineering and Biotechnology, New Delhi 110067, India

Published online: 18 June 2026

BPT-5204 is a comparatively weak culm genotype, traditionally widely cultivated in South India. Through comprehensive phenotypic characterization, yield assessment, and evaluation of key agronomic parameters in the mutant population of BPT-5204, lines TI-17 and TI-26 were identified as strong culm mutants, exhibiting enhanced culm strength and reduced lodging tendency, thereby holding potential utility for developing lodging-resistant, high-yielding rice varieties (Potupureddi et al. 2021; Balakrishnan et al. 2025). Strong culm is a crucial agronomic trait directly linked to rice yield. It is a complex trait influenced by various factors such as pushing resistance, cross-section modulus (CSM), cellulose content, culm-morphology, culm diameter and length as well as genetic and environmental factors. The strong culm trait in rice is an indispensable trait that prevents biotic and abiotic stress in rice plants (Wang et al. 2024; Guha et al. 2024; Nomura et al. 2021). Weak culms in high-yielding rice cultivars are prone to lodging, resulting in significant grain yield losses. Therefore, there is a need to transfer genes or quantitative trait loci (QTL) associated with strong culm.

Currently, few quantitative trait loci (QTL)/genes such as Strong Culm 2 (*SCM2*) (Ookawa et al. 2010) also known as *APO1* (*Aberrant panicle organization1*), *SCM3* (*OsTB1*) (Yano et al. 2015) etc. have been identified for strong culm. However, only a few markers for strong culm have been validated and utilized to bred rice. Genomics advancements have led to the development of various NGS-based rapid trait mapping approaches viz. QTL-seq, MutMap, BSA-seq, Indel-seq, Association mapping etc. (Gokulan et al. 2024a; Magar et al. 2024; Vishwakarma et al. 2024; Hake et al. 2023; Wang et al. 2023; Singh et al. 2022; Majeed et al. 2022; Varshney et al. 2020; Tribhuvan et al. 2018; Takagi et al. 2013). The availability of reference genome sequences has accelerated the identification of genomic variations and the mapping of genes associated with target traits. These sequencing and mapping approaches, coupled with updated pipelines, have improved the identification of genomic loci/QTLs with high resolution and accuracy in a more efficient and time-effective manner (Liu et al. 2024; Zhao et al. 2023). MutMap and its variants have facilitated the identification of causal genes in rice for traits such as grain quality, grain shape, magnesium uptake, panicle exertion, early flowering, root system architecture, resistance to bacterial blight and yellow stem borer (Gokulan et al. 2024a, b; Rao et al. 2025; Ballichatla et al. 2024; Magar et al. 2024; Hake et al. 2023; Kobayashi et al. 2023; Huang et al. 2022; Wang et al. 2018). Modified MutMap has been reported in case of finding the causal alleles for floury endosperm in rice (Zhang et al. 2023; Wang et al. 2018). The QTLs obtained from bi-parental linkage mapping population using recombinant inbred lines are labour and time-intensive for identification of genes. Therefore, we adopted MutMap approach where wild type parent, BPT-5204 (weak culm) crossed with its stabilized mutant, TI-17 (strong culm) and developed F_2 population which used for identification of candidate regions underlying strong culm traits. The experimental workflow for elucidating the candidate region of the strong culm trait is illustrated in Fig. 1.

Materials and methods

Population development and phenotyping for strong culm traits

Two rice genotypes namely, BPT-5204, a mega-variety having weak culm and TI-17, a strong culm ethyl methane sulphonate (EMS) mutant of BPT-5204 were deployed in the present study (Potupureddi et al. 2021). The mutant, TI-17 and BPT-5204 were crossed to generate F_1 generation, true heterozygote F_1 plant was raised (Supplementary Fig. S1) and F_2 seeds were collected. The F_2 seeds were sown in the nursery and 25 days old seedlings were transplanted in rows with 20 plants per row following a spacing of 20 cm between rows and 15 cm between plants in a randomized block design (RBD) in wet season 2022 at ICAR-Indian Institute of Rice Research, Hyderabad, India. The 262 individuals of F_2 mapping population were subjected to strong culm related traits viz. pushing resistance (N/m^2), and culm diameter (mm), along with and yield related traits viz. single plant yield (g), panicle weight (g), days to flowering (DFF), plant height (PH), tillers per plant and reproductive tillers per plant. The culm diameter was measured using a vernier calliper (Fischer-make) at the third internode from the base of culm. The pushing resistance measurement was carried out using a prostrate tester (Daiki DIK-7401) by keeping at an angle of 45° to the plant's stem at seven days after heading. Finally, the pushing resistances (culm strength) were calculated for each plant (N/m^2) by using the formula: Culm strength (N/m^2) = (test reading/40) × 1000)/ Number of tillers (Potupureddi et al. 2021; Yadav et al. 2017). Cross-section modulus was measured at seven days after heading by viewing in cross-sectional area in the middle of the internode for the F_2 extremes, calculated as $(\pi/32) \times (a_1^3 b_1 - a_2^3 b_2)/a_1$ where a_1 is the outer diameter of the minor axis in an oval cross-section, b_1 is the outer diameter of the major axis in an oval cross-section, a_2 is the inner diameter of the minor axis in an oval cross-section, and b_2 is the inner diameter of the major axis in an oval cross-section (Mulsanti et al. 2018). The section area at the second internode for the strong and weak culm extremes was calculated, and yield correlation was computed. The yield related traits were recorded as mentioned by Padmashree et al. 2023. Pearson

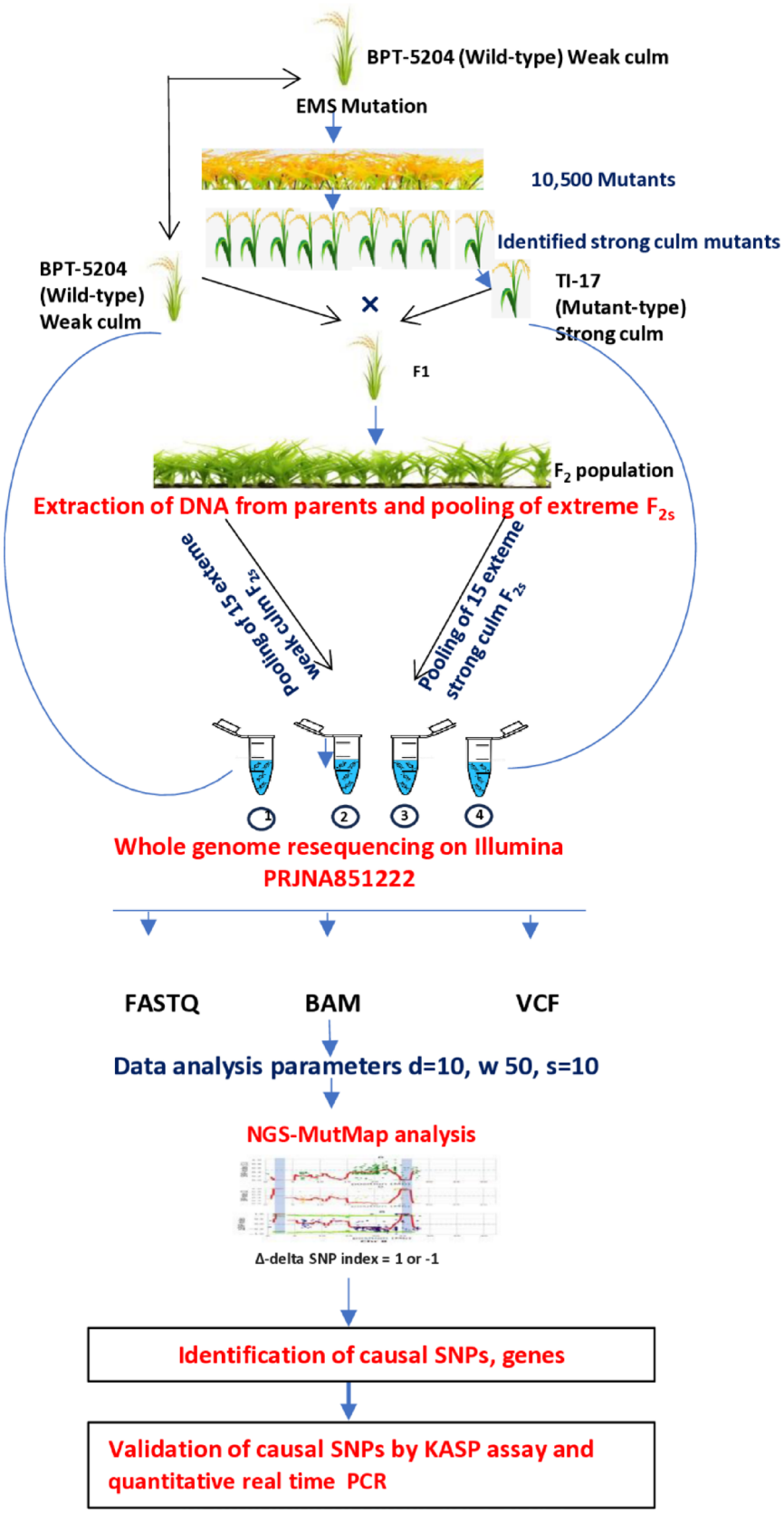


Fig. 1 Flowchart of experimental set-up for identification of strong culm candidate alleles

correlation analysis using the morphological data was carried out in R software employing the "*corrplot*" package and SPSS package. The trait inheritance for culm diameter and pushing stress was calculated using Chi square test.

Study of histological parameters

The culms of BPT-5204, TI-17, one of the weakest culm segregant (P35), and one of the strongest culm segregant (P250) from F_2 population of TI-17 × BPT-5204 were harvested seven days after heading from base. The 100 µm samples (at second internode from culm base) were fixed in 2.5% glutaraldehyde in 0.1 M phosphate buffer (pH 7.2) for 24 h at 4 °C and post-fixed in 1% in aqueous osmium tetroxide for 4 h. The samples were dehydrated in series of graded alcohols and dried to critical point with CPD (EMS 850) unit/vacuum desiccation for 35–45 min to ensure complete drying of specimens. The dried samples were mounted over the stubs with double-sided carbon conductivity tape, and a thin layer of heavy metal (gold) was coated over the samples using an automated sputter coater (Model-JEOL JFC-1600) for 3 min and scanned under Scanning Electron Microscope (SEM-Model: JOEL-JSM 5600) at required magnifications as per the standard procedures at RUSKA Lab's College of Veterinary Science, PVNR TVU, Rajendranagar, Hyderabad, India (Lakshman 2019; Bozzola and Russel 1999).

MutMap analysis: genomic DNA isolation, pooling of extreme bulks based on strength of culm and whole genome resequencing

Genomic DNA was isolated from the leaf of F_2 population of TI-17 × BPT-5204 and its parents using a modified cetyl- trimethyl ammonium bromide (CTAB) method (Doyle and Doyle 1987). The procedure in modified CTAB method included excision of leaf from plant which placed in small zip lock cover which immersed in liquid nitrogen. Further, 100 mg of plant tissue crushed in liquid nitrogen and ground into a fine powder. This is followed by cell lysis using a freshly prepared CTAB buffer (2% cetyl trimethyl ammonium bromide, 1.4 M NaCl, 100 mM Tris-HCl pH 8.0, and 20 mM EDTA). To prevent oxidation of polyphenols, β-mercaptoethanol (1% v/v) is added immediately before use. The powdered tissue is mixed with pre-warmed (65 °C) CTAB buffer and incubated for upto 30 min with intermittent mixing. Purification is achieved by adding two third volume of chloroform: isoamyl alcohol (24:1) to extraction buffer, followed by centrifugation at 13,000 × *g* for 10 min at 4 °C. The upper aqueous phase containing DNA is carefully transferred to a new tube. Genomic DNA is then precipitated using ice-cold isopropanol (1 volume) and incubated at − 20 °C for overnight. After centrifugation, the DNA pellet is washed with 70% ethanol, and the supernatant discarded. Finally, the pellet is air-dried briefly and resuspended in 100 µL of TE (Tris-EDTA) buffer. Further, RNase A (10 µg/mL) is added to remove RNA contaminants, yielding high-quality DNA suitable for downstream molecular applications. Quality of DNA was assessed by Nanodrop 2000 spectrophotometer as well as by 0.8% agarose gel electrophoresis (Gumi et al. 2018. To make bulks, equimolar genomic DNA (~1 µg) of 15 strong culms (mutant-type) and 15 weak culms (wild-type) genotypes of F_2 population were pooled and sequenced using Illumina HiSeq 2500 platform (Illumina, United States) at Eurofins Pvt. Ltd. Bangalore with a 30× genome coverage, resulting in ~ 10 GB of data per sample. Quality checks on the reads were conducted using FastP v0.20.1 and Trimmomatic v0.39. Poor-quality reads were filtered out, and potential adapter contamination was removed. Iterative trimming was carried out to ensure a mean base Phred quality score above 30 in 10 kb sliding windows. Reads shorter than 40 bp after trimming and orphan single-end reads were discarded. The high-quality short reads were mapped to the *Oryza sativa indica* (*Oryza sativa Indica* cultivar 93 − 11; ftp://ftp.ensemblgenomes.org/pub/plants/release51/fasta/oryza_indica/dna/Oryza_indica.ASM465v1.dna.toplevel.fa.gz) reference genome using BWA tool (Li and Durbin 2010), and variant calls generated with with bcftools v1.9. These variant call format (vcf) files generated from bcftools v1.9 were processed through the QTL seq pipeline (Sugihara et al. 2022) to detect reliable causal SNPs. The Paired-end sequence reads from the bulked DNA of the F_2 progeny were mapped to the same reference genome, and SNPs were classified as homozygous (delta SNP index ≥ 0.9) or heterozygous (delta SNP index between 0.3 and 0.6). Regions of the genome with clusters of SNPs showing the delta SNP index close to 1 were identified, and all SNPs within these regions were considered potential causal mutations. To create delta SNP index plot regression lines, SNP indices were calculated using a sliding window of 50 consecutive SNPs with a step size of 10 SNPs with read depth of 10X. The genomic position for each averaged Δ-delta SNP index value was defined as the midpoint between the first and tenth SNP within the window. Delta SNP-index values across the genome were plotted based on confidence intervals across the 12 rice chromosomes (Abe et al. 2012; Magar et al. 2024; Gokulan et al. 2024a). SNP index in MutMap is calculated at high and low bulks using the formula: SNP index (at position) equals count of alternate base/ count of aligned total reads. The delta

SNP-index was calculated by subtraction of SNP-index of high bulk from the SNP-index of low bulk. The functional annotation of the candidates and possible effects of the identified SNPs were inferred using SnpEff v4.3.0, an open-source program (Cingolani et al. 2012).

Validation of strong culm linked allele/s using kompetitive allele specific PCR (KASP) assay in F_2 mapping population

The delta SNP index was meticulously analyzed at the p95 and p99 intervals across the chromosomes. The SNPs chosen for validation through KASP were identified based on allelic differences and functional significance, with those having a delta SNP index close to 1 being designated as candidate SNPs. These candidate SNPs were located within genes known to be important for strong culm. The SNP indices, positions, and functional annotations were thoroughly examined, and genes with SNP indices near 1.0 were selected for further study. The KASP assays were designed for specific alleles by extracting the 50 bp upstream and downstream sequences using rice databases such as RAP-DB (https://rapdb.dna.affrc.go.jp/) and RGAP (http://rice.uga.edu/) (Table S1). Eighteen KASP assay were designed by LGC genomics (Teddington, UK; www.lgcgenomics.com). The KASP assays were conducted in PCR (BioRad CFX™ 384-well format, USA) using F_2 mapping population (262 individuals) of TI-17 × BPT-5204. The assays performed in a 384-well plate containing 10 µL reaction volume, consisting of 5 µL 2X KASP Master Mix, 0.14 µL KASP primer mix, and 4.86 µL genomic DNA (10 ng/µL) performed on the Bio-Rad CFX™ system, with a 384 well set-up and plate reader. KASP (Kompetitive Allele-Specific PCR) touchdown PCR is a two-step thermal cycling method designed for improvement of specificity and yield in SNP genotyping. It minimizes non-specific primer binding during early amplification cycles. The protocol begins with a hot-start activation at 94 °C for 15 min for activation of Taq polymerase. This is followed by a touchdown phase of 10 cycles, each consisting of 94 °C for 20 s and an annealing/extension step starting at 61 °C and decreasing by 0.6 °C per cycle to 55 °C. This gradual reduction guarantees preferential binding of perfectly matched primers in early cycles. The final amplification phase includes 26 cycles at 94 °C for 20 s and 55 °C for 60 s. Next, for data capture, reactions are cooled to 30 °C. The combined annealing-extension step simplifies the touchdown cycling. If fluorescence signals are weak, 3–12 additional cycles must be added to enhance amplification and for improving genotype clustering accuracy (Alvarez-Fernandez et al. 2021).

Quantitative real time (qRT) PCR studies for validation of genes associated with strong culm

In order to validate the gene/s associated with strong culm, identified from MutMap data, primers were designed using the Quant Prime tool (quantprime.mpimp-golm.mpg.de) (Magar et al. 2024). Two strong culm genotypes viz. TI-17 and TI-26 (NBPGR Registration No. INGR20079) along with weak culm cultivar, BPT-5204, were used in this analysis (total three genotypes). The plants were harvested at panicle initiation stage and 100 mg fresh culm tissue collected at second internode of culm and total RNA was isolated using TRIZOL reagent. Complementary DNA (cDNA) was prepared by employing the protocol of SuperScript® III cDNA synthesis protocol (Invitrogen, India) following manufacturer's instruction. The designed primers for real-time PCR and candidate gene coding sequences are depicted (Table S2). The relative expression level analysis of target transcripts was performed using 18 S rRNA and GAPDH as the endogenous control. For each biological sample, qPCR amplification was performed with two independent biological replicates and three technical replicates. For each transcript in the samples, the comparative $2^{\wedge-\Delta\Delta Ct}$ method (Livak and Schmittgen 2001) involving standard error mean was used for calculation of normalized fold changes (Gumi et al. 2018; Schmittgen and Livak 2008). Statistical analysis was performed in Microsoft Excel v. 21.

Results

Evaluation of strong culm related traits and statistical correlation

The F_2 population obtained from the cross of TI-17 and BPT-5204 was evaluated for pushing resistance and culm diameter. Based on these traits, the genotypes were classified as weak, intermediate, and strong culm. The F_1 generation from the TI-17 × BPT-5204 cross showed weak culm characteristics, suggesting that the strong culm trait is inherited recessively. In the F_2 generation, dominance epistasis was observed, resulting in a segregation ratio of 12 (180 intermediate): 3 (62weak culm): 1 (20 strong culm) for culm diameter and 12 (184intermediate): 3 (53 weak culm): 1 (25 strong culm) for pushing resistance, indicating that the strong culm is controlled by the interaction of recessive genes (Table 1). The culm diameters recorded were 5.83 mm for BPT-5204 and 8.68 mm for TI-17 (Fig. 2A). Similarly, pushing resistances of 12.83 (N/m^2) for BPT-5204 and 27.8 (N/m^2) for TI-17 were noted (Fig. 2B). Within the F_2 population, the culm diameter varied from 4.02 to 9.64 mm, while pushing resistance ranged from

Table 1 Chi square analysis identifies genetic inheritance for culm diameter and pushing resistance using F_2 mapping population of TI-17×BPT 5204

Trait	Phenotype class			Population size (*n*)
	Weak culm	Intermediate culm	Strong culm	
Culm diameter	180	62	20	262
Chi-square (for 12:3:1)	5.56*			
Pushing resistance	184	53	25	262
Chi-square (for 12:3:1)	5.64*			

*: Significant at 0.05 *p* value, Table Chi-square value at 2 df is 5.991

5.00 to 34.39 (N/m^2) (Table S3, S4, and S5). The population distribution followed a polygenic trait curve, exhibiting a positively skewed distribution for both pushing resistance and culm diameter (Fig. 3). Additionally, pushing resistance showed a positive correlation with culm diameter (+0.74) and single panicle weight (+0.262) (Table S6).

Scanning electron microscopy of culm microstructures

The electron microscopic parameters obtained for culm wall thickness, sclerenchyma thickness, xylem vessel diameter, xylem vessel protective layer thickness between parents, TI-17 and BPT-5204 along with F_2 contrasting segregants (Table 2; Fig. 4A–D). The culm wall thickness, sclerenchyma thickness, and xylem vessel sclerenchyma thickness were found to be higher in the strong culm mutant, TI-17, and an F_2 segregant resembling TI-17 (referred to as P250) when compared to their wild type counterpart with weak culms, BPT-5204, and the F_2 segregant resembling BPT-5204 (designated as P35). In contrast, the xylem vessel diameter was less in TI-17 and P250 when compared to BPT-5204 and P35.

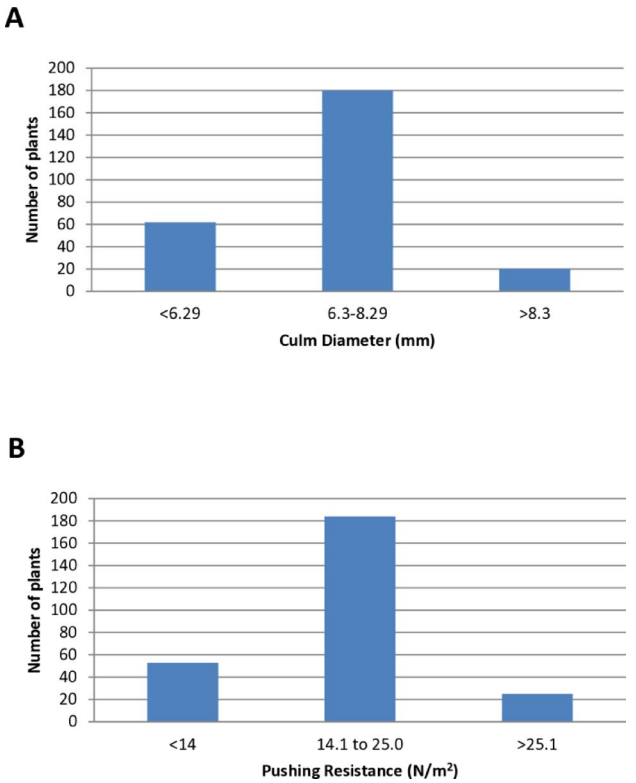


Fig. 3 F_2 population of TI-17×BPT-5204 exhibiting normal distribution pattern for cum strength parameters (**A**). culm diameter (**B**). pushing resistance

Table 2 Comparative study of culm strength parameters using scanning electron microscopy

Parameters	TI-17	BPT-5204	F_2 segregants	
			P250 (TI-17 like)	P35 (BPT-5204 like)
Culm wall thickness (µm)	373.00	243.00	333.00	245.00
Sclerenchyma thickness (µm)	43.00	18.00	40.00	18.00
Xylem vessel diameter (µm)	44.53	55.06	39.94	69.15
Xylem vessel sclerenchyma thickness (µm)	9.40	6.00	11.10	7.70

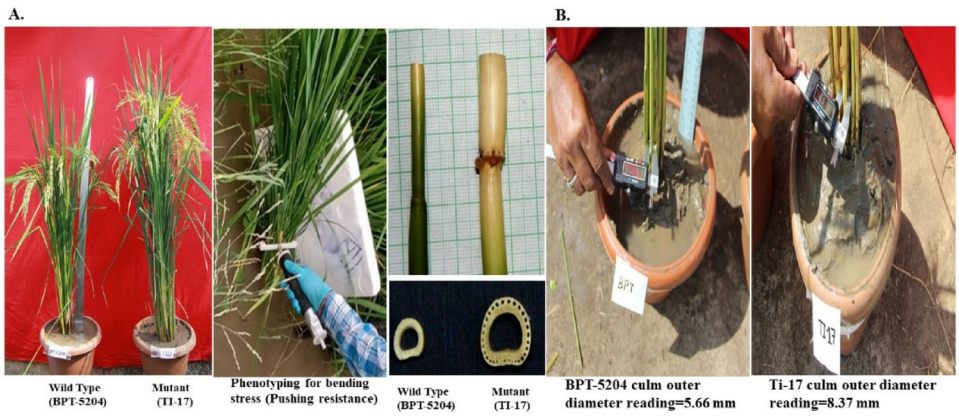


Fig. 2 Comparison of weak culm and strong culm parents for pushing resistance and culm diameter (**A**). Stature of weak culm parent (BPT-5204) and strong culm parents (TI-17) along with phenotyping for pushing resistance (**B**). Phenotyping of culm diameter in terms of thickness with vernier caliper

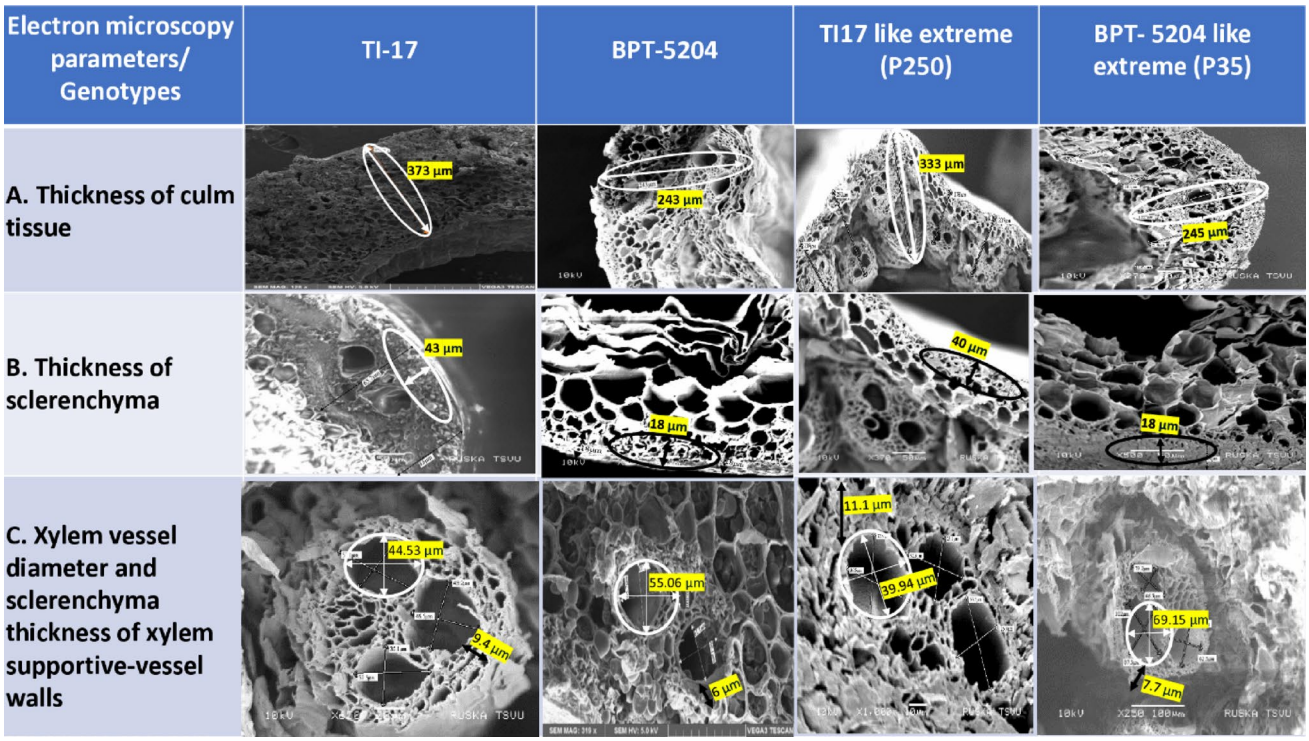


Fig. 4 Histological study of culm tissue of weak culm and strong culm genotypes using electron microscope. Pictorial image depicts: **A** Culm wall thickness **B** Sclerenchyma tissue thickness, **C** Xylem vessel diameter and sclerenchyma thickness of xylem supportive-vessel walls

MutMap data statistics

A total of 30.32 million, 30.95 million, 30.31 million, and 30.10 million paired-end (PE) reads were generated for the mutant-type bulk, wild-type bulk, TI-17, and BPT-5204, respectively. The alignment of cleaned and filtered reads derived from BPT-5204 to the reference genome assembly of indica 93−11 resulted in a mapping rate of 98.85%, facilitating the development of a reference-guided assembly for BPT-5204. Similarly, mapping of cleaned and filtered reads to the indica genome yielded a mapping rate of 98.95% with 95.70% genome coverage for TI-17. The cleaned and filtered reads generated from both the wild-type bulk and the mutant-type bulk were aligned to BPT-5204, achieving mapping rates of 98.91% (95.74% genomic coverage) and 98.93% (96.8% genomic coverage), respectively. The total length of the consensus obtained across all groups and parents was 430 Mb. The total number of single nucleotide polymorphisms (SNPs) identified were 90,255, 86,923, 117,625, and 112,559 for the mutant-type bulk, TI-17, wild-type bulk, and BPT-5204, respectively.

Genomic regions underlying strong culm

To identify the causal SNPs associated with culm strength, the SNPs obtained from the mutant-type bulk (strong culm phenotype) and wild-type bulk (weak culm phenotype) were compared with those from the wild-type parent, BPT-5204. The delta SNP index for each SNP position was calculated, retaining those with a delta SNP index of 1.0 for subsequent analysis. This study identified three MutMap regions located on chromosome 3 (253 SNPs, spanning 32.00–34.43 Mb), chromosome 4 (109 SNPs, spanning 18.14–18.52 Mb), and chromosome 8 (260 SNPs, spanning 25.0–27.00 Mb) (Fig. 5; Table S7). Following the annotation of 622 synonymous SNPs, 101 SNPs were genic while remaining intergenic. Out of 101 genic SNPs, 84 were intronic, while 17 were in the coding and untranslated region of gene (three on chromosome 3, one on chromosome 4 and 13 on chromosome 8), located within 10 different genes (Table 3). On chromosome 3, three candidate genes were identified namely, *Os03g0788800* (SNP Chr3:32784713; encodes a Zinc finger protein with a RING/FYVE/PHD-type domain), *Os03g0793500* (SNP Chr3:33000663; encodes Casein kinase I), and *Os03g0798200* (SNP Chr3:33270702; encodes a RING ubiquitin E3 ligase). On chromosome 4, a single SNP (Chr4: 18493093) was located within *Os04g0378575*, which encodes an NBS-LRR protein. In the analysis of chromosome 8, thirteen non-synonymous SNPs were observed across eight genes. Out of eight candidate genes of chromosome 8, five candidate genes namely, *Os08g0522700* (SNP Chr8:25984270; BTB/POZ-like domain containing protein), *Os08g0523100* (Chr8:26014173; BTB/POZ-like domain containing protein), *Os08g0148300* (chr8:2774013;

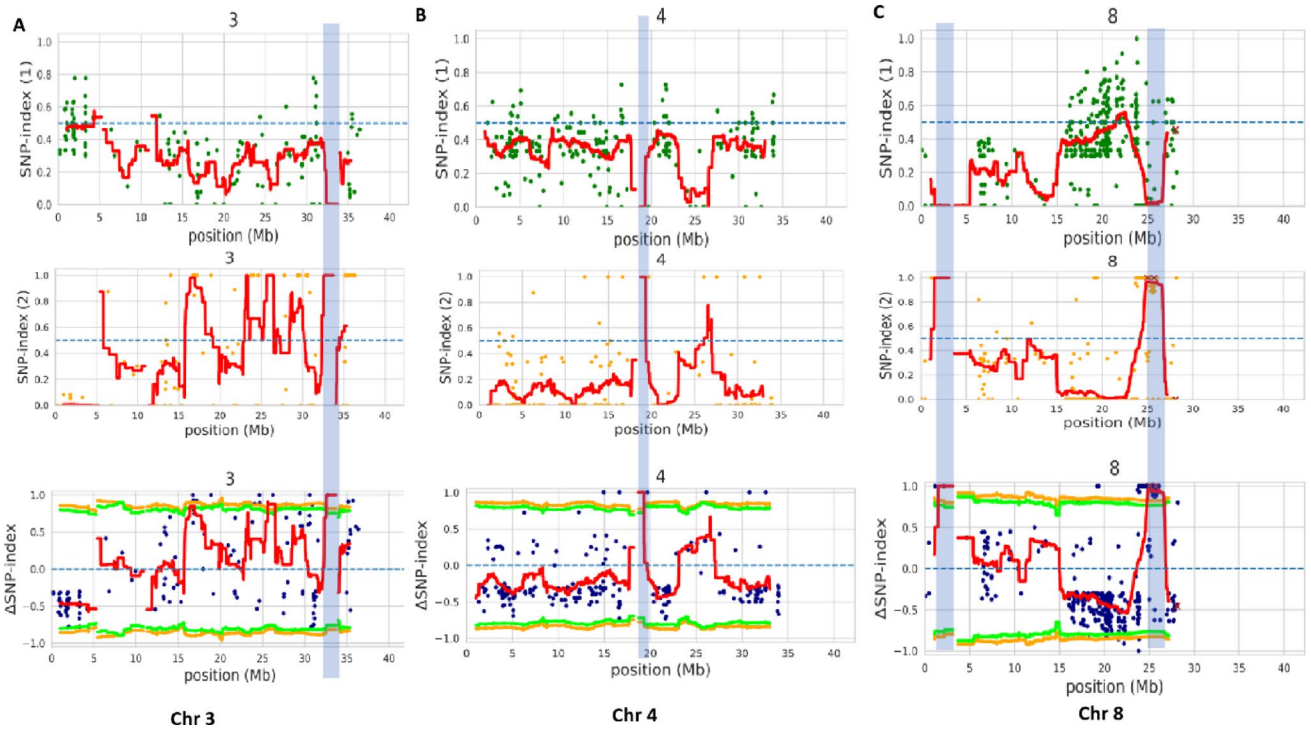


Fig. 5 MutMap identifies genomic regions governing strong culm on chromosome 3, 4 and 8. The X and Y axes depict the chromosomal position (Mb) and delta SNP index respectively. The red line depicts mean SNP-index, orange line depicts 99% confidence interval of the simulated delta SNP-index, green lie depicts 95% confidence interval of the simulated delta SNP-index

Table 3 List of causal SNPs with SNP index 1 identified by MutMap in the different genes governing culm strength

SN	Wild-type allele	Mutant-type allele	SNP position	Region	Gene	Description
1	T	A	chr3:32784713	exon	Os03g0788800	Zinc finger, RING/FYVE/PHD-type domain containing protein
2	A	G	chr3:33000663	exon	Os03g0793500	Casein kinase I
3	A	C	chr3:33270702	exon	Os03g0798200	RING Ub E3 ligase
4	A	C	chr4:18493093	exon	Os04g0378575	NBS-LRR protein
5	C	T	chr8:2322684	3_prime UTR	Os08g0141700	Pectinesterase inhibitor domain containing protein
6	T	A	chr8:2322797	3_prime_UTR		
7	T	C	chr8:25984270	exon	Os08g0522700	BTB/POZ-like domain containing protein
8	C	T	chr8:26014173	exon	Os08g0523100	BTB/POZ-like domain containing protein
9	A	G	chr8:26245439	3_prime UTR	Os08g0527300	Peptidase C19, ubiquitin carboxyl-terminal hydrolase 2 domain containing protein
10	A	T	chr8:26247367			
11	T	C	chr8:26247371			
12	A	G	chr8:26248706	exon		
13	T	C	chr8:2774013	3_prime UTR	Os08g0148300	Conserved hypothetical protein
14	A	C	chr8:2889743	3_prime UTR	Os08g0150200	F-box domain, cyclin-like domain containing protein
15	A	G	chr8:2889748			
16	C	G	chr8:2912538	5_prime UTR	Os08g0150600	F-box domain, cyclin-like domain containing protein
17	T	G	chr8:2940100	3_prime UTR	Os08g0151000	Similar to Myb-like DNA-binding domain

conserved hypothetical protein), *Os08g0150600* (chr8: 2912538; F-box domain, cyclin-like domain containing protein) and *Os08g0151000* (chr8:2940100; similar to Myb-like DNA-binding domain), containing a single SNP while two genes, *Os08g0141700* (pectinesterase inhibitor domain containing protein) and *Os08g0150200* (F-box domain, cyclin-like domain containing protein) had two SNPs. The gene, *Os08g0527300* encodes peptidase C19, ubiquitin carboxyl-terminal hydrolase 2 domain containing protein had four SNPs (one in exon and three in 3' UTR).

Table 4 Co-segregation analysis of KASP8_9 using F_2 mapping population of TI-17×BPT 5204 for culm strength

Phenotype Class	Trait		Number of common F_2 segregants displaying phenotype	Allele type exhibited by F_2 segregants			Co-segregation of allele with phenotype
	Pushing resistance	Culm diameter		strong culm allele (Mutant-type)	Weak culm allele (Wild-type)	Intermediate allele (Heterozygous-type)	
Strong culm	25	20	17	16	–	1	16/17 (94.11%)
Weak culm	53	62	49	–	49	–	49/49 (100%)
Intermediate	184	80	134	5	61	68	68/134 (50.74%)
Total	262	262	200				

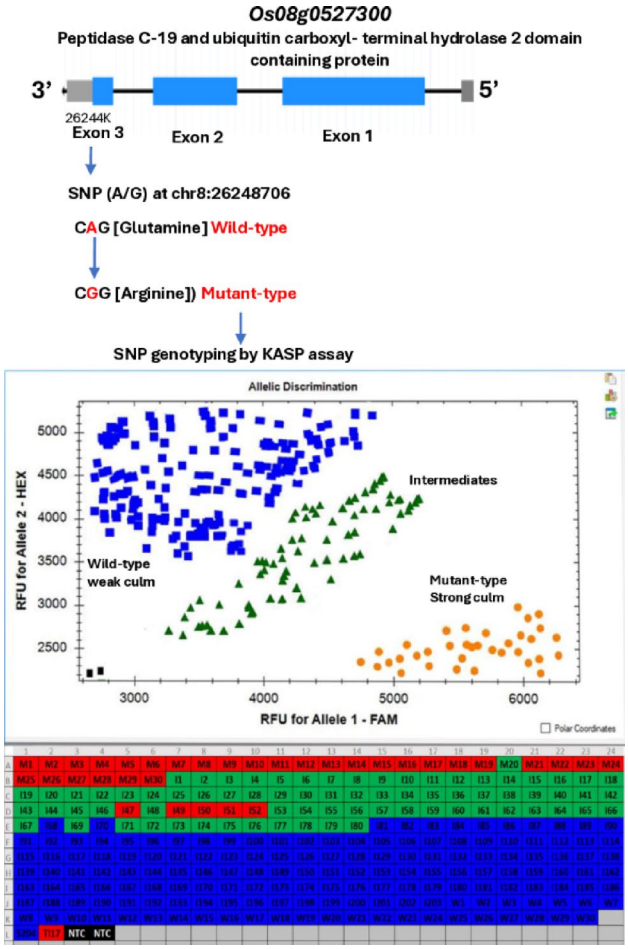


Fig. 6 Kompetitive allele specific primer-PCR depicting KASP8_9 exhibiting co-segregation with strong culm using F_2 population of TI-17×BPT-5204 Blue colour indicates the intermediate type allele, orange colour indicates the mutant-type allele and green colour wild-type alleles

Validation of strong culm linked allele through kompetitive allele-specific PCR (KASP) assay

To validate the causal SNPs associated with culm strength, we performed a KASP assay using 18 designed primers targeting coding regions of 14 candidate genes (Table S1). We selected a total of 18 SNPs from three genomic regions: three from chromosome 3, one from chromosome 4 and 13 from chromosome 8. Among the 18 KASP markers, KASP8_9 showed significant co-segregation with the culm strength trait in the F_2 population derived from TI-17 × BPT-5204. Based on our analysis of pushing resistance and culm diameter from a population of 262 individuals, we identified 200 individuals who exhibited consistent phenotypes. This group included 17 individuals with strong culm, 49 individuals with weak culm, and 134 individuals with intermediate phenotypes. Upon genotyping with KASP8_9, we found that out of the 17 strong culm F_2 segregants, 16 displayed the strong culm allele (mutant-type allele), while one genotype showed the intermediate allele. Similarly, all 49 weak culm F_2 segregants exhibited the weak culm allele. Among the 134 individuals with intermediate phenotypes, 68 genotypes were heterozygous, 61 exhibited the weak culm allele (wild-type allele), and five displayed the strong culm allele (mutant-type allele). The results are summarized in Tables 4 and S8. A pictorial representation of the KASP plate for this population is shown in Fig. 6.

Validation of gene expression through quantitative real-time PCR (qRT-PCR)

Additionally, we designed a primer targeting the exonic region of the gene *Os08g0527300* (KASP8_9), which encodes a protein containing the peptidase C19 and ubiquitin carboxyl-terminal hydrolase 2 domains and conducted a qRT-PCR analysis using cDNA from TI-17, BPT-5204, and TI-26. The results indicated a reduced expression of the gene *Os08g0527300* in BPT-5204 (weak culm parent), while an increased expression was observed in its mutants TI-17 and TI-26 (Fig. 7).

Discussion

Mutation breeding is an effective approach for exploring genomic alterations, identifying new traits, and developing cultivars. In this study, we utilized the stabilized strong culm mutant TI-17, derived from a weak culm wild-type parent BPT-5204. This strong culm trait in rice is essential to mitigate lodging under various biotic and abiotic stresses.

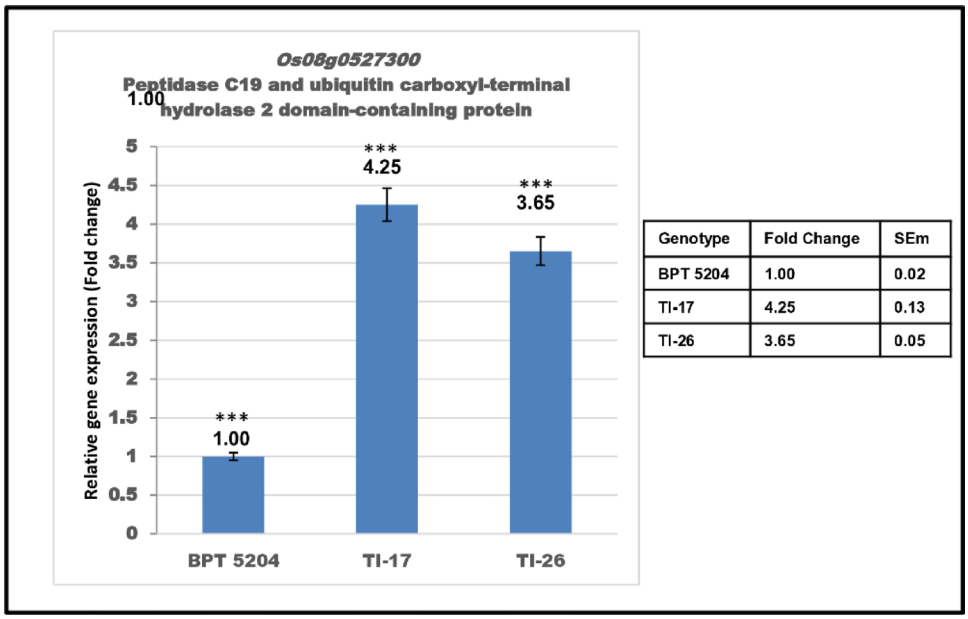


Fig. 7 Reduced expression of gene Os08g0527300 in BPT-5204 compared to TI-17 and TI-26

The F_1 progeny resulting from the cross between TI-17 and BPT-5204 exhibited a weak culm phenotype similar to that of the wild-type parent, indicating that the trait follows recessive gene action. The F_2 population derived from the TI-17 × BPT-5204, demonstrated dominance epistasis, where the strong culm trait is controlled through the interaction of homozygous recessive alleles of genes. In rice, several traits are governed by recessive alleles, such as blast resistance, which is controlled by the gene *pi66(t)* (Liang et al. 2016), and bacterial blight resistance, governed by genes *xa5* and *xa13* (Huang et al. 2016; Antony et al. 2010). The F_2 population of TI-17 × BPT-5204 exhibited a normal distribution skewed towards the strong culm trait, characterized by a large culm diameter and high pushing resistance. This indicates that culm strength is inherited quantitatively and involves multiple genes. Furthermore, pushing resistance showed a positive correlation with culm diameter and single panicle weight, suggesting that stronger culms can support heavier panicles, ultimately leading to higher yields. Similar observations have been noted in other studies (Vishwakarma et al. 2024; Yadav et al. 2017).

Electron microscopy of culm tissue indicated increased sclerenchyma thickness and culm wall thickness in the mutant TI-17 and its F_2 segregant P250, while a reduced xylem diameter in these mutants contributed to enhanced culm strength compared to the wild-type BPT-5204. These findings align with previous studies showing that thicker culm walls correlate with greater strength (Wang et al. 2017) and that smaller xylem diameters enhance water potential, thereby increasing culm strength and stiffness (de Moraes et al. 2022). A wider culm diameter with a thinner wall can optimize lodging resistance without compromising yield potential (Ookawa et al. 2010). Correlation analysis revealed that culm strength metrics, including culm diameter and pushing resistance were positively correlated with panicle weight (Zhang et al. 2016). Cross-sectional modulus analysis indicated a positive correlation between lodging resistance, culm strength, and yield traits, with higher cross-sectional modulus reflecting greater accumulation of structural carbohydrates such as lignin and cellulose, which supports increased yields as observed in our study and others (Sowadan et al. 2024; Ookawa et al. 2022; Zhang et al. 2016).

Genome sequencing in rice has facilitated sequencing-based trait mapping. The MutMap approach has identified important agronomic loci for traits such as complete panicle exsertion (Hake et al. 2023), semidwarfism, pale green leaf (Abe et al. 2012), floury endosperm (Zhang et al. 2023), white-spotted leaf (Kim et al. 2019), resistance to yellow stem borer and bacterial blight (Gokulan et al. 2024a, b) and early flowering (Rao et al. 2025) using extreme bulks of F_2 populations. In this study, we identified three novel genomic regions on chromosome 3 (32.00–34.43 Mb, covering 2.43 Mb), chromosome 4 (18.14–18.52 Mb, covering 0.4 Mb), and chromosome 8 (25.0–27.00 Mb, covering 2.0 Mb) which is differed with earlier identified genomic regions for strong culm. The allele KASP8_9 (chr8:26248706) of the *Os08g0527300* gene, which encodes a peptidase C19, ubiquitin carboxyl-terminal hydrolase 2 domain-containing protein, was strongly associated with the culm strength trait. This finding allowed us to clearly differentiate between weak and strong culm genotypes. The missense mutation (CAG[Glutamine] to CGG[Arginine]) in the gene *Os08g0527300* results in a conformational change in peptidase C19, ubiquitin carboxyl-terminal hydrolase 2 domain-containing protein of the mutant TI-17, leading

to a strong culm phenotype. The Peptidase C19, ubiquitin carboxyl-terminal hydrolase 2 domain-containing protein belongs to the peptidase C19 family and contains a ubiquitin carboxyl-terminal hydrolase domain, functioning as a deubiquitinase that removes ubiquitin from other proteins and regulates their degradation. In the context of rice, these enzymes, also known as ubiquitin-specific processing proteases (UBPs) involved in the regulation and development of stamen in rice (Wang et al. 2018). Comparative analysis with earlier reports indicated that these regions are non-overlapping with previously mapped QTLs, thereby supporting their novelty. For instance, earlier studies have identified major SC-related loci such as *SCM1* (chr1; *Gn1a*, cytokinin oxidase/dehydrogenase), *SCM2* (chr6; *ABERRANT PANICLE ORGANIZATION1* [*APO1*]) (Ookawa et al. 2010), *SCM3* (chr3; TCP domain transcription factor [*OsTB1*]) (Yano et al. 2015), and *dep1* (Dense and Erect Panicles 1; G protein γ subunit) (Wang et al. 2024) as well as QTLs for culm diameter and bending stress on Chr. 3 (21.64–24.26 Mb) and Chr. 4 (29.09–34.61 Mb) (Chigira et al. 2023). Also, in other studies candidate genes such as *OsPRR37* (response regulator receiver domain containing protein) and *OsRLCK191* (protein kinase family protein) and *LOC_Os05g48810* (DNA/J-binding protein) identified for lodging resistance (Gopi et al. 2026; Guo et al. 2021; Chigira et al. 2020). In contrast, the regions identified in our study on Chr. 3 (32.71–33.70 Mb) and Chr. 4 (18.2–20 Mb) are spatially distinct from these previously reported loci, indicating that they represent novel genomic intervals. Similarly, GWAS-based studies (Badri et al. 2024) identified marker–trait associations on chromosomes 2 and 12, along with candidate genes on Chr. 8 such as cinnamoyl-CoA reductase (CCR) and monosaccharide transporter 5. While our Chr. 8 region (24.0–27.0 Mb) lies in far to these genes, it does not overlap with their reported positions (~4.5–4.9 Mb), suggesting that the loci identified here are distinct, and therefore potentially represent new regulatory regions. Other reported loci (*OsPRR37*) and QTLs (qCT7 and qIBW7) on Chr. 7 (Guo et al. 2021; Mamidi et al. 2025) and QTLs on Chr. 5, 6, and 11 (Chigira et al. 2020; Bian et al. 2024), were not detected in our analysis, further emphasizing the uniqueness of our findings. Importantly, beyond positional novelty, this study identifies new candidate genes and allelic variants associated with SC. These include genes involved in cell wall biosynthesis and lignification (E3 ligase, Pectinesterase inhibitor domain-containing proteins) transcriptional regulation (MYB transcription factors and Zinc finger protein containing a RING/FYVE/PHD-type domain), and protein turnover (Peptidase C19 ubiquitin-specific proteases and BTB/POZ domain proteins). Taken together, while previous studies have established key loci for culm strength, our results identify previously unreported genomic regions and candidate genes in an BPT-5204 mutant background, thereby expanding the genetic architecture of strong culm. The lack of overlap with major known QTLs, combined with the identification of novel alleles and pathways, highlights the contribution of this study to uncovering new genetic determinants of culm strength for breeding applications.

Also, the other underlying genes have significant roles towards strong culm traits. The gene *Os08g0522700* and *Os08g0523100* encode to BTB/POZ domain-containing protein functions as a substrate-specific adapter within an E3 ubiquitin-protein ligase complex. This protein likely plays a role in regulating culm (stem) strength, potentially through ubiquitination and subsequent degradation of target proteins related to development, differentiation, cell wall regulation, and chromatin structure (Shalmani et al. 2021; Gingerich et al. 2005). An interesting novel allele is present in this gene imparting strong culm in rice (Jeong et al. 2023; Pla-Prats and Thomä 2022). The gene *Os08g0141700* encodes pectinesterase inhibitor domain-containing proteins (PMEIs), which primarily serve as regulators of plant cell wall structure by binding to and inhibiting pectin methylesterase (PME) enzymes, ultimately affecting pectin levels. The protein *Os08g0150200*, containing an F-box domain and a cyclin-like domain, is a component of the E3 ubiquitin ligase complex, specifically the SCF (Skp1-Cullin-F-box) type. This complex is involved in the ubiquitin-26 S proteasome pathway, where it tags target proteins for degradation. The F-box domain is crucial for substrate recognition, and the cyclin-like domain likely plays a role in protein-protein interactions within the complex and with the target protein (Yang et al. 2023). This is a novel report not reported in strong culm rice scenario. On chromosome 8, we identified the gene *Os08g0151000*, which encodes a transcription factor with a Myb-like DNA-binding domain specifically belonging to the SHAQKYF class. This protein is characterized by a highly conserved motif, SH[AL]QKY[RF], located at its C-terminal end functions as a transcription factor, and is involved in regulating gene expression associated with strong culm (stem) development in rice (Zhang et al. 2023). In prior investigations, the *STRONG2* gene, which encodes mannan synthase, facilitated the deposition of mannan sugars in the cell wall, resulting in an increased culm diameter and improved lodging resistance. The expression of the *STRONG2* gene is activated by the *MYB61* transcription factor (Zhao et al. 2025). The gene *Os08g0151000* in rice encodes a protein containing a Myb-like DNA-binding domain,the gene *Os08g0501500* in rice encodes a protein containing an EGF-like domain, structurally similar to the epidermal growth factor (EGF) domain, playing a role in cell growth, development, and signaling pathways in various organisms. In rice, function of this gene associated with

strong culm development, which is crucial for plant architecture and resistance to lodging (Verica et al. 2003).

The other candidate genes located on chromosome 3 and 4 regions demonstrate associations with pathways that govern cell wall biosynthesis, vascular development, and protein turnover. For instance, the candidate gene *Os03g0788800* on chromosome 3 encodes a Zinc finger protein containing a RING/FYVE/PHD-type domain, which is linked to pronounced culm characteristics in rice. Previous research by Wang et al. (2016) identified a missense mutation in the zinc finger domain of *OSCESA7* (*LOC_Os10g32980*), which adversely affects cellulose biosynthesis and plant growth in rice. In our analysis, a mutation in this gene produced a robust strong culm in the mutant. Furthermore, the candidate gene *Os03g0798200* encodes an E3 ligase that contributes to enhanced culm strength. In a separate study, the gene *OsBBI1* encoding E3 ligase, was associated with increased cell wall thickness and the accumulation of phenolic compounds, thereby improving tolerance to biotic stress, particularly rice blast (Li et al. 2011). Another gene, *Os03g0793500*, which encodes casein kinase I, exhibited a strong culm in mutants. Li et al. (2024) revealed that *DTG1*, which encodes casein kinase I, improves resistance to lodging by enhancing culm thickness through direct interaction with Grain Width 2 (*GW2*) in rice. Additionally, a mutation in the gene *Os04g0378575*, which encodes an NBS-LRR protein on chromosome 4, also contributes to strong culm development. NBS-LRR proteins recognize effectors and initiate effector-triggered immunity (ETI). Zheng et al. (2021) demonstrated that *Bph14*, which encodes an NB-LRR protein, interacts with transcription factors *OsWRKY46* and OsWRKY72. This interaction enhances the expression of the callose synthase gene, resulting in callose deposition in sieve tubes and the accumulation of cellulose, hemicellulose, and lignin in cell walls, thereby strengthening the culm. The involvement of these genes collectively support cell wall biosynthesis, lignification, transcriptional regulation, and stress-response pathways in governing the strong culm phenotype, thereby providing support for candidate regions identified on chromosomes 3 and 4 in addition to chromosome 8.

The SEM analysis revealed that the strong culm mutant TI-17 and its segregant P250 exhibited increased sclerenchyma thickness and culm wall thickness, along with reduced xylem vessel diameter compared to the wild type. These anatomical features are directly associated with enhanced mechanical support: thicker sclerenchyma and culm walls increase load-bearing capacity, while reduced xylem diameter contributes to improved tissue compactness and stiffness. These observations are consistent with earlier reports linking culm wall thickening and vascular architecture with improved culm strength and lodging resistance (Zhang et al. 2016; Wang et al. 2017; Li et al. 2020; de Moraes et al. 2022). These structural modifications were quantitatively supported by mechanical analysis. The increased cross-sectional modulus (CSM) observed in the mutants indicated superior resistance to bending stress and lodging, providing a direct functional link between anatomical changes and culm biomechanics. In our study, mutant TI-17 shown higher value (24.36 mm^3) for CSM over its wild-type (7.84 mm^3). Various reports have pointed out regarding higher CSM meaning greater accumulation of structural carbohydrates, viz. lignin and cellulose, and non-structural carbohydrates in the culm (Sowadan et al. 2024; Ookawa et al. 2022; Zhang et al. 2016). Furthermore, correlation analysis showed that key strength-related traits such as culm diameter (CD) and pushing resistance (PR) were positively associated with panicle weight (PW) ($r = 0.63$ and 0.64), suggesting that enhanced mechanical strength contributes to yield stability rather than imposing a trade-off. These phenotypic and mechanical traits were also observed with the identified candidate genomic regions associated with strong culm on chromosomes 3, 4, and 8. For instance, genes encoded to E3 ligase, Pectinesterase inhibitor domain-containing proteins, Peptidase C19, ubiquitin carboxyl-terminal hydrolase 2 domain containing protein involved in lignin biosynthesis and cell wall reinforcement provide a mechanistic explanation for increased sclerenchyma thickness and culm wall development. Similarly, regulatory components such as Zinc finger protein containing a RING/FYVE/PHD-type domain, Myb-like DNA-binding domain and MATH-BTB proteins are implicated in signaling networks that coordinate growth, stress responses, and structural development (Shi et al. 2019; Ullah et al. 2023).

In particular, the identification of missense mutations in genes related to ubiquitin-mediated protein degradation and developmental regulation suggests altered control of cell wall deposition and vascular differentiation, which aligns with the observed anatomical changes. Thus, the genomic findings provide a causal framework linking gene function to tissue architecture and, ultimately, to enhanced mechanical strength (Nakamichi et al. 2020; Wang et al. 2023). Overall, the integration of SEM-based anatomical observations, cross-sectional modulus analysis, and MutMap-derived candidate genes supports a coordinated model in which genetic variation modulates cell wall biosynthesis and vascular patterning, leading to improved culm strength, lodging resistance, and yield stability in the mutants.

In summary, culm strength and culm diameter are critical for determining the strong culm trait in rice. The novel candidate genes identified through MutMap, confirmed by SNP genotyping and quantitative expression analysis, highlight the essential role of Peptidase C-19, ubiquitin carboxyl-terminal hydrolase 2 domain containing protein

in shaping the recessive trait and the dominant inhibitory epistasis of strong culm. The identified KASP marker associated with strong culm traits can be deployed in molecular breeding studies for improvement of strong culm especially in the realm of climate resilience. Also, the marker can be deployed for location specific breeding viz. for coastal areas where lodging is a major issue because of unpredicted winds and storms. Future research may explore genome-editing effects of Peptidase C-19, with the potential release of strong culm cultivars offering significant value for developing lines resistant to biotic and abiotic stresses.

Supplementary Information The online version contains supplementary material available at https://doi.org/10.1007/s12892-026-00363-1.

Acknowledgements The authors thank to Director, ICAR-IIRR for providing field and lab facilities. The authors also thank Dr. Jyothi Badri and Dr. C. N. Neeraja for providing the necessary instruments used in the study. The mutant rice lines deployed in the study were developed and identified as a part of the CSIR-funded XII five-year plan project PLOMICS and the FBR project 'Towards product development in rice using mutants that have traits of agronomic importance.

Author contributions MSM and RVS conceived the study; MSM and KMB planned and designed the experiments; PKG, AAH, GP, NDM, BV, MK performed phenotyping, validation experiments, and genotyping. MSM contributed to the genetic material. GCG, MJ, AS and RM executed scripts and analyzed MutMap data. AAH, KMB, MSM and PKG drafted manuscript. MSM, HKP, RVS, SRM, DVRP, DVL, ACS, KMB and AAH critically revised manuscript. All authors reviewed and approved the submission.

Funding The research was supported as part of the Department of Science and Technology-Science and Engineering Research Board (DST-SERB), Government of India, Core Research Grant EMR/2017/004527 to Dr. Sheshu Madhav Maganti (ICAR-IIRR) and from XIIth five-year plan project PLOMICS, Council of Scientific and Industrial Research, New Delhi to Dr. Ramesh V. Sonti (CSIR-CCMB).

Data availability The cleaned reads from the Mutant-type bulk, Wild-type bulk, TI-17 and BPT-5204 have been submitted to the NCBI SRA database with the BioProject ID: PRJNA851222 (Accession nos. SRX15805121, SRX15805120, SRX15805119, SRX15805118).

Declarations

Conflict of interest The authors declare that they have no conflict of interest.

Ethical approval We declare that these experiments complied with the ethical standards in India.

Consent to participate Not applicable.

Clinical trial number Not applicable.

References

Abe A, Kosugi S, Yoshida K et al (2012) Genome sequencing reveals agronomically important loci in rice using MutMap. Nat Biotechnol 30(2):174–178

Alvarez-Fernandez A, Bernal MJ, Fradejas I et al (2021) KASP: a genotyping method to rapid identification of resistance in Plasmodium falciparum. Malar J 20(1):16

Antony G, Zhou J, Huang S et al (2010) Rice *xa13* recessive resistance to bacterial blight is defeated by induction of the disease susceptibility gene Os-11N3. Plant Cell 22(11):3864–3876

Badri J, Padmashree R, Anilkumar C et al (2024) Genome-wide association studies for a comprehensive understanding of the genetic architecture of culm strength and yield traits in rice. Front Plant Sci 14:1298083

Balakrishnan D, Badri J, Padmavathi G et al (2025) Genetic stock bulletin No. 131. ICAR-Indian institute of rice research, Hyderabad

Ballichatla S, Gokulan CG, Barbadikar KM et al (2024) Impairment in a member of *AP2/ERF* and *F-box* family protein enhances complete panicle exsertion, an economically important trait in rice. J Exp Bot 28:erae244

Bian Z, Cao D, Zou Y et al (2024) Genetic dissection of major rice QTLs for strong culms and fine mapping of qWS5 for breeding application in transplanted system. Rice 17(1):43 https://doi.org/10.1186/s12284-024-00723-x

Bozzola JJ, Russell LD (1999) Electron microscopy: principles and techniques for biologists. Jones & Bartlett Learning

Chigira K, Kojima N, Yamasaki M et al (2020) Landraces of temperate japonica rice have superior alleles for improving culm strength associated with lodging resistance. Sci Rep 10(1):19855

Chigira K, Yamasaki M, Adachi S et al (2023) Identification of novel quantitative trait loci for culm thickness of rice derived from strong-culm landrace in Japan. Omachi Rice 16(1):4. https://doi.org/10.1186/s12284-023-00621-8

Cingolani P, Platts A, Wang le L et al (2012) A program for annotating and predicting the effects of single nucleotide polymorphisms, SnpEff: SNPs in the genome of *Drosophila melanogaster* strain w1118 iso-2 iso-3. Fly (Austin) 6(2):80–92

de Moraes DH, Mesquita M, Graciano-Ribeiro D et al (2022) The effect of xylem vessel diameter on potential hydraulic conductivity in different rice stem longitudinal positions. Flora 295:152147

Doyle JJ, Doyle JL (1987) A rapid DNA isolation procedure for small quantities of fresh leaf tissue. Phytochemic Bullet

Gingerich DJ, Gagne JM, Salter DW et al (2005) Cullins 3a and 3b assemble with members of the broad complex/tramtrack/bric-a-brac (BTB) protein family to form essential ubiquitin-protein ligases (E3s) in Arabidopsis. J Biol Chem 280(19):18810–18821

Gokulan CG, Bangale U, Balija V et al (2024a) Multiomics-assisted characterization of rice-Yellow Stem Borer interaction provides genomic and mechanistic insights into stem borer resistance in rice. Theoret Appl Genet 137(6):122

Gokulan CG, Deb S, Gaur N et al (2024b) *Xanthomonas oryzae* pv. *oryzae* type-III effector TAL9b targets a broadly conserved disease susceptibility locus to promote pathogenesis in rice. bioRxiv 2024-05

Gopi P, Hake AA, Ballichatla S et al (2026) Converging QTL mapping with MutMap identifies novel genomic regions associated with strong culm in rice (*Oryza sativa* L). Planta 263(3):61

Guha PK, Magar ND, Kommana M et al (2024) Strong culm: a crucial trait for developing next-generation climate-resilient rice lines. Physiol Mol Biol Plants 30(4):665–686

Gumi AM, Guha PK, Mazumder A et al (2018) Characterization of *OglDREB2A* gene from African rice (*Oryza glaberrima*), comparative analysis and its transcriptional regulation under salinity stress. 3 Biotech 8(2):91

Guo Z, Liu X, Zhang B et al (2021) Genetic analyses of lodging resistance and yield provide insights into post-green-revolution breeding in rice. Plant Biotechnol J 19(4):814–829

Hake AA, Ballichatla S, Barbadikar KM et al (2023) Combined strategy employing MutMap and RNA-seq reveals genomic regions and genes associated with complete panicle exsertion in rice. Mol Breed 43(9):69

Huang S, Antony G, Li T et al (2016) The broadly effective recessive resistance gene *xa5* of rice is a virulence effector-dependent quantitative trait for bacterial blight. Plant J 86(2):186–194

Huang X, Zeng X, Cai M et al (2022) The *MSI1* member *OsRBAP1* gene, identified by a modified MutMap method, is required for rice height and spikelet fertility. Plant Sci 320:111201

Jeong Y, Oh AR, Jung YH et al (2023) Targeting E3 ubiquitin ligases and their adaptors as a therapeutic strategy for metabolic diseases. Exp Mol Med 55(10):2097–2104

Kim B, Lee H, Jin Z et al (2019) Characterization and genetic mapping of white-spotted leaf *(wspl)* mutant in rice. Plant Breed Biotechnol 7(4):340–349

Kobayashi NI, Takagi H, Yang X et al (2023) Mutations in *RZF1*, a zinc-finger protein, reduce magnesium uptake in roots and translocation to shoots in rice. Plant Physiol 192(1):342–355

Lakshman M (2019) Application of conventional electron microscopy in aquatic animal disease diagnosis: a review. J Entomol Zool Stud 7(1):470–475

Li H, Durbin R (2010) Fast and accurate long-read alignment with Burrows–Wheeler transform. Bioinformatics 26(5):589–595

Li W, Zhong S, Li G et al (2011) Rice RING protein OsBBI1 with E3 ligase activity confers broad-spectrum resistance against Magnaporthe oryzae by modifying the cell wall defence. Cell Res 21(5):835–848

Li W, Wang K, Chern M et al (2020) Sclerenchyma cell thickening through enhanced lignification induced by OsMYB30 prevents fungal penetration of rice leaves. New Phytol 226(6):1850–1863

Li J, Zhou D, Li D et al (2024) The dual role of casein kinase 1, DTG1, in regulating tillering and grain size in rice. Crop J 12(6):1569–1582

Liang Z, Wang L, Pan Q (2016) A new recessive gene conferring resistance against rice blast. Rice 9(1):1–6

Liu J, Xiang D, Du Y et al (2024) Quantitative Trait Loci mapping and association analysis of solanesol content in tobacco (*Nicotiana tabacum* L). Agronomy 14(7):1370

Livak KJ, Schmittgen TD (2001) Analysis of relative gene expression data using real-time quantitative PCR and the $2^{-\Delta\Delta CT}$ method. Nat Methods 25(4):402–408

Magar ND, Barbadikar KM, Reddy V et al (2024) Genetic mapping of regions associated with root system architecture in rice using MutMap QTL-Seq. Plant Physiol Biochem 17(8):108836

Majeed A, Johar P, Raina A et al (2022) Harnessing the potential of bulk segregant analysis sequencing and its related approaches in crop breeding. Front Genet 13:944501

Mamidi A, Krishna L, Badri J et al (2025) Navigating rice culm resilience: high-throughput quantitative trait locus mapping in indica and tropical japonica derived population. Plant Sci 9:112756

Mulsanti IW, Yamamoto T, Ueda T et al (2018) Finding the superior allele of *japonica*-type for increasing stem lodging resistance in *indica* rice varieties using chromosome segment substitution lines. Rice 11(1):1–4

Nakamichi N, Kudo T, Makita N et al (2020) Flowering time control in rice by introducing Arabidopsis clock-associated PSEUDO-RESPONSE REGULATOR 5. Biosci Biotechnol Biochem 84(5):970-979 https://doi.org/10.1080/09168451.2020.1719822

Nomura T, Seki Y, Matsuoka M et al (2021) Potential of rice landraces with strong culms as genetic resources for improving lodging resistance against super typhoons. Sci Rep 11(1):15780

Ookawa T, Hobo T, Yano M et al (2010) New approach for rice improvement using a pleiotropic QTL gene for lodging resistance and yield. Nat Comm 1:132

Ookawa T, Nomura T, Kamahora E et al (2022) Pyramiding of multiple strong-culm genes originating from indica and tropical japonica to the temperate japonica rice. Sci Rep 12(1):15400

Padmashree R, Barbadikar KM, Honnappa et al (2023) Genome-wide association studies in rice germplasm reveal significant genomic regions for root and yield-related traits under aerobic and irrigated conditions. Front Plant Sci 14:1143853

Pla-Prats C, Thomä NH (2022) Quality control of protein complex assembly by the ubiquitin–proteasome system. Trends Cell Biol 32(8):696–706

Potupureddi G, Balija V, Ballichatla S et al (2021) Mutation resource of Samba Mahsuri revealed the presence of high extent of variations among key traits for rice improvement. PLoS ONE 16(10):e0258816

Rao D, Sai TN, Gokulan CG et al (2025) Omics-driven identification of candidate genes and SNP markers in a major QTL controlling early heading in rice. bioRxiv 03

Schmittgen TD, Livak KJ (2008) Analyzing real-time PCR data by the comparative C(T) method. Nat Protoc 3(6):1101–1108

Shalmani A, Huang YB, Chen YB et al (2021) The highly interactive BTB domain targeting other functional domains to diversify the function of BTB proteins in rice growth and development. Int J Biol Macromol 192:1311–1324

Shi C, Ren Y, Liu L et al (2019) Ubiquitin specific protease 15 has an important role in regulating grain width and size in rice. Plant Physiol 180(1):381–391

Singh V, Sinha P, Obala J et al (2022) QTL-seq for the identification of candidate genes for days to flowering and leaf shape in pigeonpea. Heredity 128(6):411–419

Sowadan O, Xu S, Li Y et al (2024) Genome-wide association analysis unravels new quantitative trait loci (QTLs) for eight lodging resistance constituent traits in rice (*Oryza sativa L*). MDPI Genes 15(1):105

Sugihara Y, Young L, Yaegashi H et al (2022) High-performance pipeline for MutMap and QTL-seq. Peer J 10:e13170

Takagi H, Abe A, Yoshida K et al (2013) QTL-seq: rapid mapping of quantitative trait loci in rice by whole genome resequencing of DNA from two bulked populations. Plant J 74(1):174–183

Tribhuvan KU, Sandhya, Kumar K et al (2018) MutMap: a versatile tool for identification of mutant loci and mapping of genes. Indian J Plant Physiol 23:612–621

Ullah U, Mao W, Abbas W et al (2023) *OsMBTB32*, a MATH-BTB domain-containing protein that interacts with *OsCUL1s* to regulate salt tolerance in rice. Funct Integrat Genomics 23(2):139

Varshney RK, Sinha P, Singh VK et al (2020) 5Gs for crop genetic improvement. Curr Opin Plant Biol 56:190–196

Verica JA, Chae L, Tong H et al (2003) Tissue-specific and developmentally regulated expression of a cluster of tandemly arrayed cell wall-associated kinase-like kinase genes in Arabidopsis. Plant physiol 133(4):1732-1746 https://doi.org/10.1104/pp.103.028530

Vishwakarma MK, Bhati PK, Kumar U et al (2024) Genetic dissection of value-added quality traits and agronomic parameters through genome-wide association mapping in bread wheat (*T. aestivum* L). Front Plant Sci 15:1419227

Wang D, Qin Y, Fang J et al (2016) A missense mutation in the zinc finger domain of OSCESA7 deleteriously affects cellulose biosynthesis and plant growth in rice. PLoS ONE 11(4):e153993

Wang J, Wang R, Wang Y et al (2017) *Short and Solid Culm/RFL/APO2* for culm development in rice. Plant J 91(1):85–96

Wang DH, Song W, Wei SW et al (2018) Characterization of the ubiquitin C-terminal hydrolase and ubiquitin-specific protease families in rice (*Oryza sativa*). Front Plant Sci 9:1636

Wang H, Lu H, Yang Z et al (2023) Characterization of lodging variation of weedy rice. J Exp Bot 74(5):1403-1419 https://doi.org/10.1093/jxb/erac480

Wang X, Han L, Li J et al (2023) Next-generation bulked segregant analysis for Breeding 4.0. Cell Rep 42(9):113039

Wang Y, Wang M, Yan X et al (2024) The *DEP1* mutation improves stem lodging resistance and biomass saccharification by affecting cell wall biosynthesis in rice. Rice 17(1):35

Yadav S, Singh UM, Naik SM et al (2017) Molecular mapping of QTLs associated with lodging resistance in dry direct-seeded rice (*Oryza sativa* L). Front Plant Sci 8:1431

Yang X, Yang G, Wei X et al (2023) OsAAP15, an amino acid transporter in response to nitrogen concentration, mediates panicle branching and grain yield in rice. Plant Sci 330:111640

Yano K, Ookawa T, Aya K et al (2015) Isolation of a novel lodging resistance QTL gene involved in strigolactone signaling and its pyramiding with a QTL gene involved in another mechanism. Mol Plant 8(2):303–314

Zhang WJ, Wu LM, Ding YF et al (2016) Top-dressing nitrogen fertilizer rate contributes to decrease culm physical strength by reducing structural carbohydrate content in *japonica* rice. J Int Agric 15(5):992–1004

Zhang L, You R, Chen H et al (2023) A New SNP in *AGPL2*, associated with floury endosperm in rice, is identified using a modified MutMap method. Agronomy 13(5):1381

Zhao R, Liu B, Wan W et al (2023) Mapping and characterization of a novel adult-plant leaf rust resistance gene *LrYang16G216* via bulked segregant analysis and conventional linkage method. Theoret Appl Genet 136(1):1

Zhao Y, Wang X, Gao J et al (2025) The MYB61–STRONG2 module regulates culm diameter and lodging resistance in rice. J Integr Plant Biol 67(2):243–257

Zheng X, Zhu L, He G (2021) Genetic and molecular understanding of host rice resistance and *Nilaparvata lugens* adaptation. Curr Opin Insect Sci 45:14–20

Publisher's note Springer Nature remains neutral with regard to jurisdictional claims in published maps and institutional affiliations.

Springer Nature or its licensor (e.g. a society or other partner) holds exclusive rights to this article under a publishing agreement with the author(s) or other rightsholder(s); author self-archiving of the accepted manuscript version of this article is solely governed by the terms of such publishing agreement and applicable law.